PIER C

(Received 14 September 2024, Accepted 29 October 2024, Scheduled 5 November 2024)

# Monopole Antenna Loading Parasitic Metal Pillar Element with Suppression of Beam Upwarping to Improve Omnidirectional Radiation in Broadband

Jiemin Jing, Wenquan Cao*, Hong Xue, Chuang Wang, Yangkun Zhu, Yixin Tong, and Huangshu Zhou

*College of Communications Engineering, Army Engineering University of PLA, Nanjing 210007, China*

**ABSTRACT:** Due to the presence of finite ground, the radiation pattern of a monopole antenna will upwarp, thereby affecting the communication quality in the horizontal direction. Loading parasitic metal pillar elements near monopole antenna is a common beam control method. In this paper, an inverted monopole antenna is used as the source antenna to analyze the effect and band of beam upwarping suppression in wide band. The working principle and parameter analysis of elements are also discussed. This antenna can achieve 1–24° of suppression from 360 to 570 MHz. At the same time, keeping the un-roundness almost unchanged, the horizontal plane gain is increased by 0.53–1.74 dB. The omnidirectional pattern is improved, which provides a valuable candidate for vehicle communication.

## 1. INTRODUCTION

As well known, antenna serves as a terminal for transmitting and receiving electromagnetic waves. Depending on specific requirements, users can select antennas that operate within the desired band and offer varying radiation characteristics. For instance, in vehicle communication, monopole antenna is often used as vehicle antenna because of its omnidirectional radiation characteristics [1, 2]. However, due to the limitations by the shape and size of the mounting carrier, the upwarping of the beam and the distortion of the radiation pattern will appear [3–7].

According to the theoretical analysis, the radiation characteristics of monopole antenna can be attributed to the interaction between the space wave radiated by the antenna and the surface wave induced on the ground [4]. On the one hand, by changing the ground and loading the structures on the ground plane, the surface wave can be adjusted to improve the radiation characteristics. In order to reduce the edge diffraction of the ground plane and restrain the deterioration of the radiation pattern, resistance and absorbing materials are loaded on the ground plane [8, 9]. The upwarping of the beam is suppressed by loading a resonant slot on the ground [10, 11]. In [12, 13], mushroom structures and ring EBG structures are loaded on the ground surface to realize the regulation of surface waves and smooth the radiation direction pattern of the monopole antenna. Loading ring dielectric structures and ring EBG structures to improve the un-roundness of monopole antenna placed off-center has been studied [14, 15]. In work [16], mushroom structures are uniformly loaded to the ground surface of a double conical antenna. This approach effectively suppresses the upwarping of the beam by the properties of the mushroom structure outside the bandgap. The above researches have realized the regulation of surface waves, but the theoretical analysis and machining are more complicated.

On the other hand, adjusting the space wave can realize beam regulation effectively. A classical method of regulating space wave is loading parasitic metal pillar elements near the source antenna (SA). In [17], it is proposed for the first time to realize directional beam control by loading parasitic metal pillar elements near SA to form a parasitic array, that is the classic Yagi antenna structure. Since then, the researchers have conducted a more in-depth analysis of parasitic array working principles [18–22]. In addition, the omnidirectional radiation pattern is improved by loading parasitic elements around the monopole antenna uniformly [23]. On this basis, the directional beam can be realized in the horizontal plane by loading adjustable impedance on the parasitic element [24–29]. Compared with the surface wave control method, the loading structure and theoretical analysis method are simpler. However, in previous studies, the antenna with narrow operating band is mainly used as SA, and the operation band of elements on the wide band is rarely introduced.

In order to study the suppression effect of parasitic metal pillar elements in wide band, an inverted conical antenna with wide operating bandwidth is used as the SA in this paper. At the same time, the effect and band of elements on beam upwarping suppression are analyzed under different numbers, sizes, and loading positions, so as to obtain better horizontal radiation characteristics in wide band.

## 2. ANTENNA DESIGN AND OPERATING PRINCIPLE

### 2.1. Antenna Configuration

The configuration of the proposed antenna is shown in Fig. 1. The overall structure of the antenna is mainly composed of three

* Corresponding author: Wen-Quan Cao (cao_wenquan@163.com).

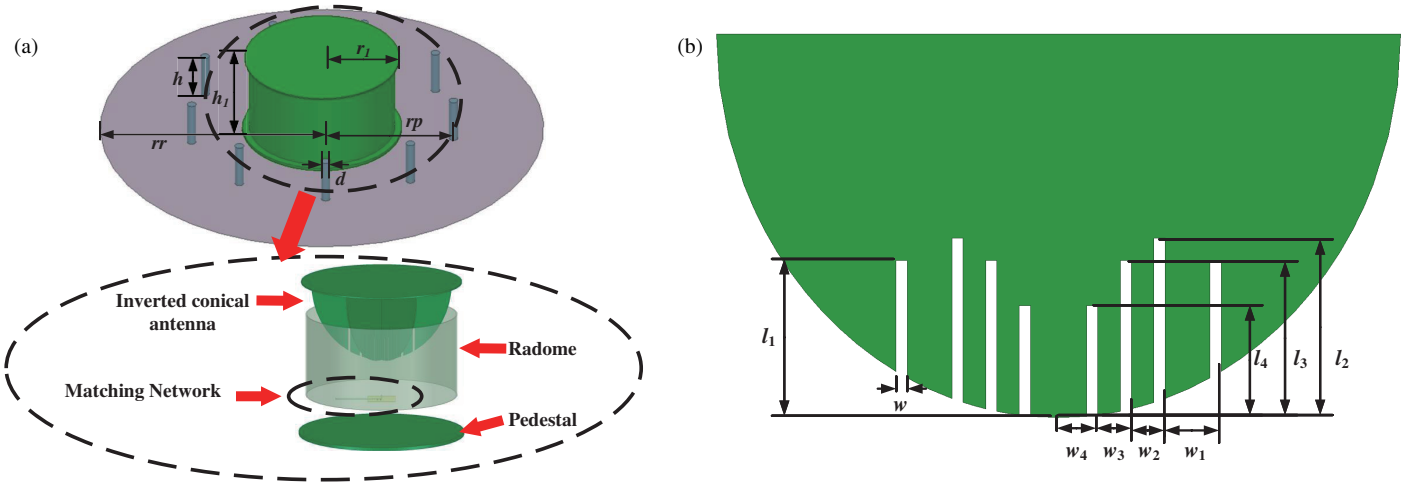


**FIGURE 1**. (a) Configuration of the proposed antenna. (b) The structure of inverted conical antenna.

parts: SA, ground plane, and parasitic metal pillar element. The SA is an inverted conical monopole antenna covering 250 to 530 MHz with top loading and slots.

The loaded parasitic metal pillar elements play the role of controlling the space wave. By uniformly loading elements in a ring pattern, it can suppress beam upwarping while improving omnidirectional radiation of the antenna in the horizontal plane. The geometric parameters of the proposed antenna are mainly given in Table 1.

**TABLE 1**. Parameters of the proposed antenna.

| parameters | values | parameters | values |
|---|---|---|---|
| $h$ | 100 mm | $rp$ | 120 mm |
| $h_1$ | 180 mm | $r_1$ | 180 mm |
| $rr$ | 500 mm | $d$ | 10 mm |
| $l_1$ | 70 mm | $l_2$ | 80 mm |
| $l_3$ | 70 mm | $l_4$ | 50 mm |
| $w_1$ | 15 mm | $w_2$ | 15 mm |
| $w_3$ | 15 mm | $w_4$ | 25 mm |
| $w$ | 5 mm | | |

## 2.2. The Operating Principle of Parasitic Metal Pillar Elements

The parasitic metal pillar element can guide the space wave radiated by SA towards the horizontal plane. For better analysis, as described in [5], the derivation of the formula is given here when the ground is infinite

$$E = E_{SA} + E_P$$

$$= \left[ I_{SA}F_{SA} + mI_PF_P \cdot \sum_{i=1}^{m} e^{i\left(A\cos\left(\varphi - \frac{2\pi i}{m}\right)\right)} \right] \cdot \frac{e^{-jkr}}{r}$$

$$= I_{SA}F_{SA}\left[ 1 + mBC\sum_{i=1}^{m} e^{i\left(A\cos\left(\varphi - \frac{2\pi i}{m}\right)\right)} \right] \cdot \frac{e^{-jkr}}{r} \quad (1)$$

$$\begin{cases} A = 2\pi\rho\sin\theta/\lambda \\ B = F_P/F_{SA} \\ C = I_P/I_{SA} \end{cases} \quad (2)$$

$I_{SA}$ is the current on SA radiation, $I_P$ the induced current on the element, and $m$ the number of elements. $F_P$ and $F_{SA}$ are the coefficients related to the size and shape of the elements and SA. The influence of the ground on radiation can be discussed as equivalent to the SA of the mirror and elements of the mirror. The series in (1) can be expanded as follows [30]

$$\sum_{i=1}^{m} e^{iA\cos\left(\varphi - \frac{2\pi i}{m}\right)} = J_0(A)$$
$$+2\sum_{k=1}^{\infty} i^{km}\cos(km\varphi)J_{km}(A) \quad (3)$$

When $m$ is big enough

$$J_0(A) \gg J_m(A) \quad (4)$$

In this case, the series of (1) can be written as

$$E = I_{SA}F_{SA}[1 + mBCJ_0(A)] \cdot e^{-jkr}/r \quad (5)$$

It can be found that improving radiation can be achieved by changing $m$, $A$, $B$, and $C$. $m$ and $B$ cannot change without altering the antenna structure. It is obvious that the performance of the antenna depends on $C$, which is a complex number. When the phase on $I_P$ is behind that on $I_{SA}$, radiation enhancement can be achieved. $C$ depends on the self-impedance and mutual impedance of all components. It can be written here as [23]

$$\begin{cases} V_{SA} = I_{SA}Z_{SA} + mI_PZ_{1S} \\ 0 = I_{SA}Z_{1S} + I_PZ_{all} \\ Z_{11} + Z_{12} + \ldots + Z_{1m} = Z_{all} \end{cases} \quad (6)$$

$$C = |C|e^{i\psi_B} = -Z_{1S}/Z_{all}$$
$$= |Z_{1S}/Z_{all}|e^{i(\pi + \psi_m + \psi_a)} \quad (7)$$

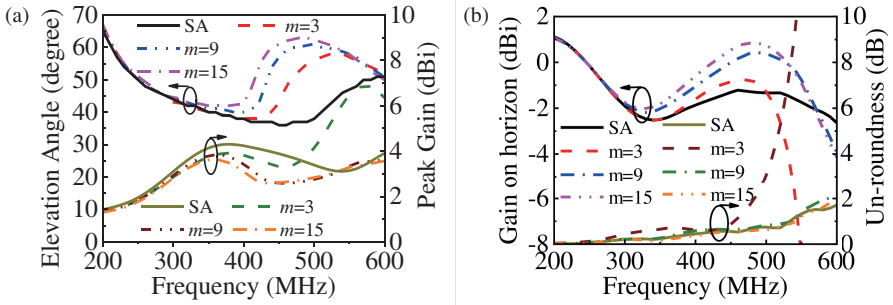


**FIGURE 2**. (a) Elevation angle and value of peak gain for the antennas with different $m$. (b) Gain and un-roundness on horizon plane of antennas with different $m$.

$Z_{11}$ is the self-impedance of elements, $Z_{1s}$ the mutual impedance between elements and SA, and if $i \neq j$, $Z_{ij}$ is the mutual impedance between elements. In previous studies [31], a half wavelength dipole antenna was used as SA, when $m = 1$ and $\rho = \lambda/4$ in the horizontal plane

$$E = I_{SA} F_{SA} \left[1 + m\,|B|\, e^{i\theta_B} C e^{i\frac{\pi \cos\varphi}{2}}\right] \cdot \frac{e^{-jkr}}{r} \qquad (8)$$

The classic conclusion can be drawn that when element is inductive, it acts as a reflector, reflecting space wave. When element is capacitive, it acts as a director, guiding space waves. In this article, it can be understood that when the element is inductive relative to SA, it can reflect space wave, causing the antenna beam to warp more significantly. However, when the parasitic element is capacitive relative to SA, it can play a role in suppressing the upwarping of the beam. By controlling the impedance changes of elements, it is possible to control the band that suppresses beam upwarping.

It should be emphasized that when $h \ll \lambda$, it can make $|Z_{all}| \gg |Z_{1s}|$ and $|B| \approx 0$, which cannot achieve the effect of space wave regulation. This also leads to the fact that tuning parameters can hardly change the lowest frequency point that has the effect of suppressing beam warping. The above formula can provide theoretical support for subsequent analysis.

### 2.3. The Effect of the Number of Parasitic Metal Pillar Elements ($m$)

As can be seen from Figs. 2 and 3, the effect of suppressing beam upwarping becomes increasingly apparent, and the gain in the horizontal plane also becomes stronger with the increase of $m$. However, the smaller $m$ in the horizontal plane makes the un-roundness increase significantly, resulting in distortion of the radiation pattern obviously in high frequency, as shown in Fig. 3. It can be thought that when $m$ is small, the elements play the role of directional beam regulation.

Combined with (1) and (4), the series in (1) cannot be ignored, and its impact becomes more pronounced as the frequency increases. So when $m$ is smaller, the gain on the horizontal plane is more obviously affected by angle $\varphi$ at high frequency.

Combined with the increase of $m$ in Fig. 4, the impedance characteristics become significantly worse. It can be concluded

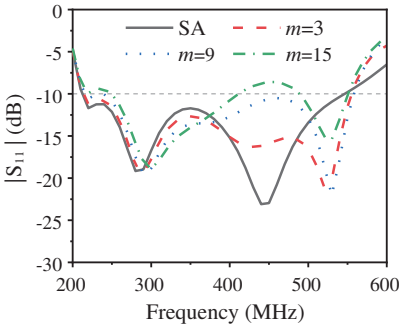


**FIGURE 3**. The reflection coefficients with different $m$.

that in order to obtain a better suppression effect of beam upwarping in wide band, it is necessary to load as many elements as possible under the condition of guaranteeing the impedance characteristics.

### 2.4. The Effect of the Loading Position of Parasitic Metal Pillar Elements ($rp$)

When the parasitic metal pillar element acts as a director, it can guide the space wave and suppress the upwarping of the beam. $rp$ is an important factor. As shown in Figs. 5 and 6, by reducing $rp$, the effect of beam upwarping suppression can be enhanced, and the operating band can be broadened. This is because the closer the distance is between the SA and elements, the stronger the regulation effect is on the space wave. Combining (5) and (7), it can be observed that as the distance between the two approaches, the mutual impedance between SA and parasitic elements increases, where $|B|$ is significantly enhanced, and the suppression effect of beam warping is significantly enhanced. In addition, the decrease in $rp$ increases the highest frequency value of the Bessel function term in the positive range in (5), that is, the highest frequency point in the band that plays a role in suppressing beam warping. The reduction of $rp$ causes a decrease in $\rho$, thereby resulting in an increase in the capacitance interval. If other variables remain constant, the field strength in the horizontal plane can be enhanced.

By observing Fig. 7, it can be found that as the distance between the SA and elements becomes closer, the impedance characteristics will deteriorate significantly. The $rp$ should be selected while ensuring that the impedance characteristics meet the required design requirements.

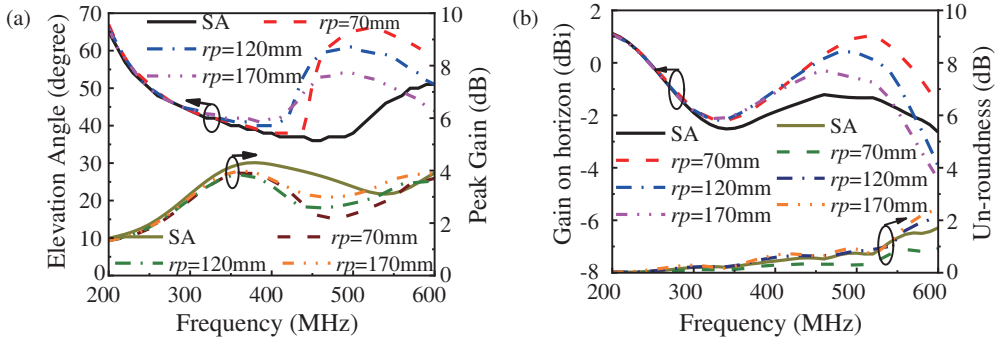


**FIGURE 4**. (a) Elevation angle and value of peak gain for the antennas with different $rp$. (b) Gain and un-roundness on horizon plane of antennas with different $rp$.

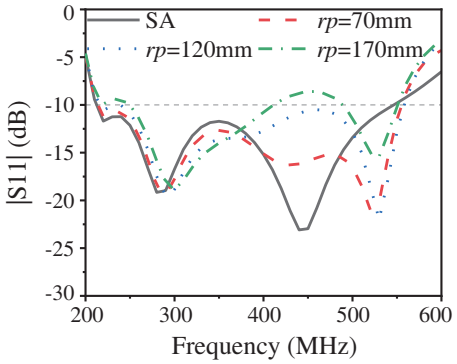


**FIGURE 5**. The reflection coefficients with different $rp$.

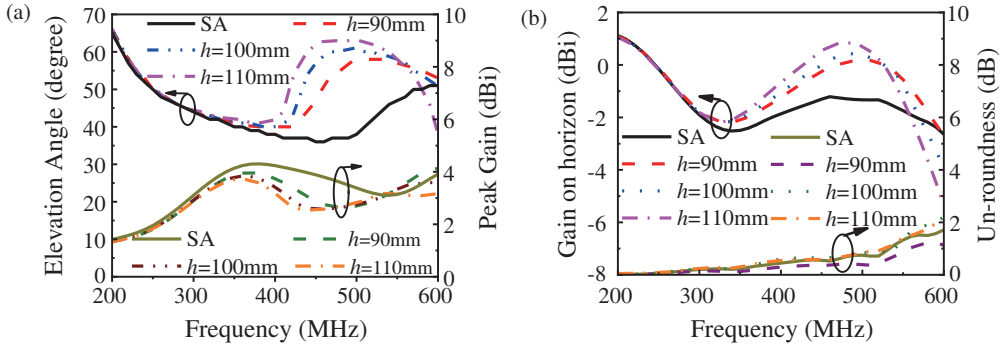


**FIGURE 6**. (a) Elevation angle and value of peak gain for the antennas with different $h$. (b) Gain and un-roundness on horizon plane of antennas with different $h$.

### 2.5. The Effect of the Size of Parasitic Metal Pillar Elements ($h$, $d$)

Changing the size of the parasitic metal pillar element can affect the effect and band of suppressing the upwarping of the beam. As illustrated in Figs. 8 and 9, with the increase of $h$, the inhibition effect of beam upwarping becomes more obvious. At the same time, it also significantly narrows the band that effectively suppresses beam upwarping.

Combining (2) and (5), it can be observed that as $h$ increases, $F_P$ increases, leading to omnidirectional radiation enhancement. However, the increase of $h$ causes the resonance point of elements to shift towards lower frequency, resulting in the highest frequency point that suppresses beam upwarping moving towards lower frequencies. Thus, the effective bandwidth is narrowed.

From (2), (5), and (7), it can be seen that as $d$ increases, $Z_{all}$ decreases, which enhances the radiation on the horizontal plane. The growth of $d$ also shifts the resonant frequency of the component towards higher frequencies, thereby expanding the bandwidth that plays a role in suppressing beam warping. The trend in Fig. 7 confirms the correctness of the theoretical analysis. Fig. 8 shows the trend of impedance characteristics under different $h$ and $d$. In the design, the influence of $h$ and $d$ should be considered comprehensively to obtain better suppression of beam upwarping in wide band.

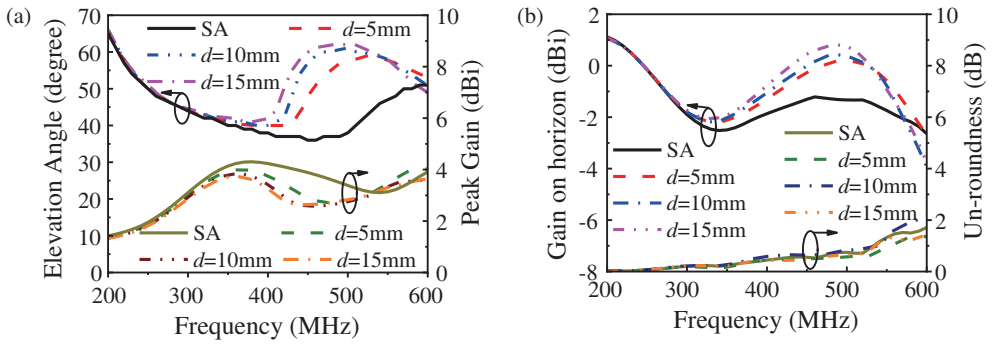


**FIGURE 7**. (a) Elevation angle and value of peak gain for the antennas with different $d$. (b) Gain and un-roundness on horizon plane of antennas with different $d$.

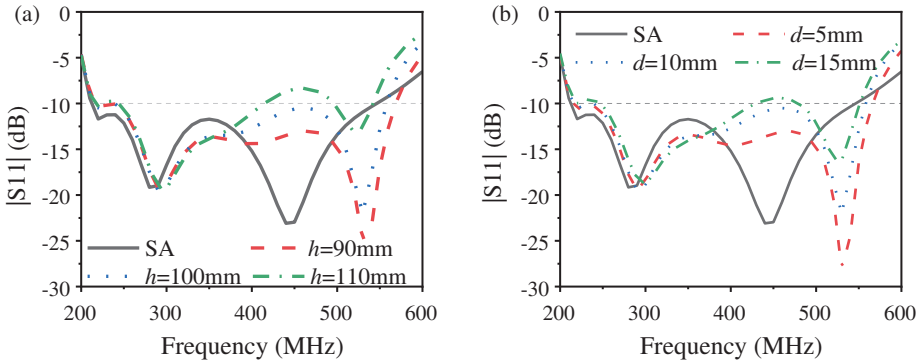


**FIGURE 8**. The reflection coefficients with different (a) $h$ and (b) $d$.

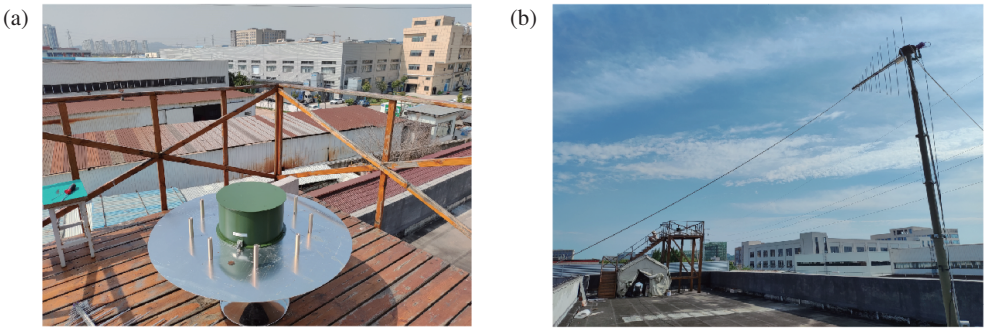


**FIGURE 9**. Photographs of (a) the proposed antenna and (b) the test site.

## 3. MEASUREMENT RESULTS AND DISCUSSION

Based on the above-mentioned analysis, the antenna is fabricated, which is shown in Fig. 9(a). Parasitic metal pillar elements are designed to be detachable. The antennas are measured and compared before and after loading the elements.

In Fig. 10, the impedance bandwidths before and after loading the elements are 250–520 MHz and 210–540 MHz. Compared to the simulation results, the measured bandwidth is noticeably narrower. External interference may lead to this deviation.

The radiation characteristics of the antennas are tested in outdoor field, as shown in Fig. 9(b). In order to clarify the effect and band of components on beam regulation, we present the main beam in the vertical plane and the radiation patterns of the horizontal plane at three frequency points, as depicted in Fig. 11. It can be observed that the beam upwarping is suppressed, and the omnidirectional radiation is enhanced af-

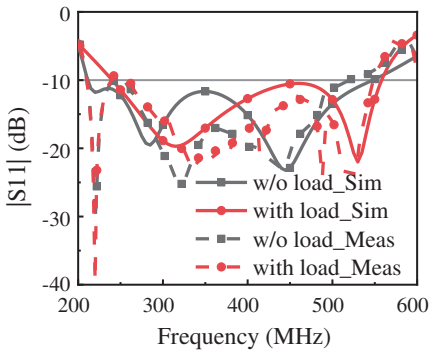


**FIGURE 10**. Simulated and measured $|S_{11}|$ of the antenna before and after loading elements.

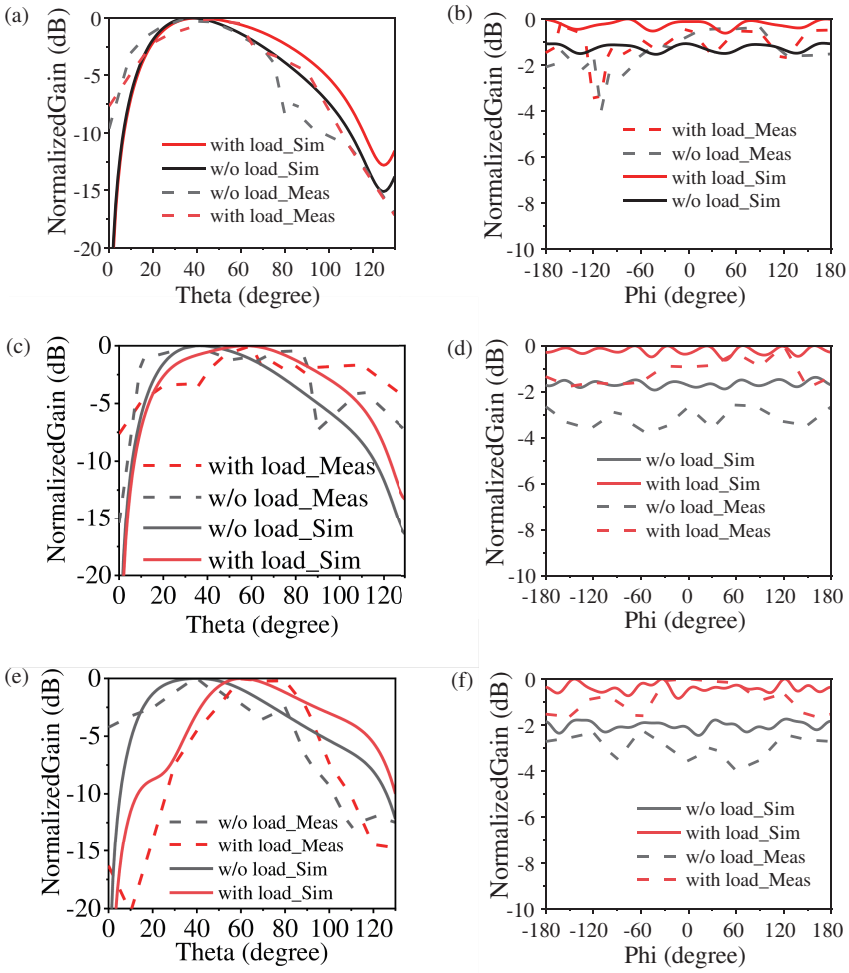


**FIGURE 11**. Simulated and measured radiation patterns of the antenna before and after loading elements. (a) 410 MHz, vertical plane. (b) 410 MHz, horizontal plane. (c) 450 MHz, vertical plane. (d) 450 MHz, horizontal plane. (e) 410 MHz, vertical plane. (f) 510 MHz, horizontal plane.

**TABLE 2**. Suppression effects of the proposed antenna.

| name | Angle of suppression (°) | Operating band (MHz) | Gain on horizon improving (dB) | Method to suppress the beam upwarping |
|---|---|---|---|---|
| [25] | 40 | 13.5% (1450–1660) | — | skirt ground + parasitic metal pillar element |
| [26] | 20 | 4% (980–1020) | 1.6 | skirt ground |
| [16] | 4–8 | 25.4% (480–620) | — | loading mushroom structure on ground |
| Sim | 1–24 | 45.2% (360–570) | 0.53–1.74 | parasitic metal pillar element |
| Meas | 5–25 | 23.7% (410–520) | 0.42–2.21 | parasitic metal pillar element |

ter loading elements, but there are discrepancies between the measured and simulation data. Taking Figs. 11(e) and (f) as an example, at 510 MHz, the simulation values for the maximum radiation direction before and after loading are 40° and 60°, respectively, while the measured values are 35° and 60°. The deviation of the measured radiation pattern may be caused by the error caused by the placement and rotation of the antenna to bemeasured. In addition, the horizontal gains of simulation and measurement are enhanced after loading the element. However, due to the electromagnetic energy of the outdoor field, the horizontal plane pattern is distorted.

Table 2 summarizes the comparison of beam upwarping suppression effects between references and simulation and measured data in wide band. It can be found that the proposed antenna has better suppression effect in wide band. The difference between the simulation and measurement is due to the limitation and influence of the outdoor environment. The corner spacing of the receiving antenna is relatively large, making it difficult to exhibit weak beam warping suppression effects in the low band. In the high frequency band, the impedance characteristics deteriorate, resulting in distortion of the radiation pattern. However, it can still be proven that the suppres-

sion effect of loading parasitic metal pillar element is much improved in wide band.

## 4. CONCLUSION

This paper presents simulated and measured results for the suppression of beam upwarping by the parasitic metal pillar element loaded near the inverted monopole antenna as SA in the wide band. The working principle and parameter analysis of the elements are discussed. Simulation results show that the proposed antenna achieves 1–24° suppression of beam upwarping from 360 to 570 MHz. In addition, the horizontal gain is increased by 0.53–1.74 dB without worsening the un-roundness. Although there are differences, the measured results can still prove the role of the elements. Therefore, this design improves the omnidirectional radiation on horizontal plane which offers application potential in vehicle communication.

## REFERENCES


[1] Webster, R., "20-70 MC monopole antennas on ground-based vehicles," *IRE Transactions on Antennas and Propagation*, Vol. 5, No. 4, 363–368, 1957.

[2] League, A. R. R., *The ARRL Antenna Book*, The League, 1949.

[3] Bardeen, J., "The diffraction of a circularly symmetrical electromagnetic wave by a co-axial circular disc of infinite conuctivity," *Physical Review*, Vol. 36, No. 9, 1482, 1930.

[4] Leitner, A. and R. D. Spence, "Effect of a circular groundplane on antenna radiation," *Journal of Applied Physics*, Vol. 21, No. 10, 1001–1006, 1950.

[5] Pozar, D. and E. Newman, "Analysis of a monopole mounted near an edge or a vertex," *IEEE Transactions on Antennas and Propagation*, Vol. 30, No. 3, 401–408, 1982.

[6] Weiner, M., "Monopole element at the center of a circular ground plane whose radius is small or comparable to a wavelength," *IEEE Transactions on Antennas and Propagation*, Vol. 35, No. 5, 488–495, 1987.

[7] Chu, A. W. C., S. A. Long, and D. R. Wilton, "The radiation pattern of a monopole antenna attached to a conducting box," *IEEE Transactions on Antennas and Propagation*, Vol. 38, No. 12, 1907–1912, 1990.

[8] Griffin, D., "Monopole antenna method of diagnosing the effectiveness of ground plane edge scattering elimination techniques," in *1982 Antennas and Propagation Society International Symposium*, Vol. 20, 223–226, 1982.

[9] Wang, R. W., "Reduction of the edge diffraction of a circular ground plane by using resistive edge loading," Ph.D. dissertation, University of Michigan, Ann Arbor, MI, USA, 1985.

[10] Wen, Y. and P.-Y. Qin, "Yagi-Uda monopoles with elevated-angle suppression for endfire radiation," in *2022 International Symposium on Antennas and Propagation (ISAP)*, 417–418, Sydney, Australia, Oct. 2022.

[11] Wen, Y., P.-Y. Qin, G.-M. Wei, and R. W. Ziolkowski, "Circular array of endfire Yagi-Uda monopoles with a full 360° azimuthal beam scanning," *IEEE Transactions on Antennas and Propagation*, Vol. 70, No. 7, 6042–6047, 2022.

[12] Sievenpiper, D., L. Zhang, R. F. J. Broas, N. G. Alexopolous, and E. Yablonovitch, "High-impedance electromagnetic surfaces with a forbidden frequency band," *IEEE Transactions on Microwave Theory and Techniques*, Vol. 47, No. 11, 2059–2074, 1999.

[13] Janapsatya, J. and M. Bialkowski, "Improving monopole antennas' radiation pattern by implementing a structured ground plane," in *IEEE International Symposium on Phased Array Systems and Technology*, 329–332, Boston, MA, USA, Oct. 2003.

[14] Zhang, B. and Z. N. Chen, "Radiation Pattern Roundness Improvement of Off-center Monopole Antenna Using Electromagnetic Band-gap (EBG) Structure," in *2021 IEEE International Symposium on Antennas and Propagation and USNC-URSI Radio Science Meeting (APS/URSI)*, 1313–1314, Singapore, Dec. 2021.

[15] Sheng, H. and Z. N. Chen, "Improving radiation pattern roundness of a monopole antenna placed off-center above a circular ground plane using characteristic mode analysis," *IEEE Transactions on Antennas and Propagation*, Vol. 69, No. 2, 1135–1139, 2020.

[16] Jing, J., W. Cao, C. Wang, Y. Zhu, and Y. Tong, "Application of mushroom structure to suppress upwarping of antenna pattern after grounding," in *2023 IEEE 11th Asia-Pacific Conference on Antennas and Propagation (APCAP)*, 1–2, Guangzhou, China, Nov. 2023.

[17] Yagi, H., "Beam transmission of ultra short waves," *Proceedings of the Institute of Radio Engineers*, Vol. 16, No. 6, 715–740, 1928.

[18] Walkinshaw, W., "Theoretical treatment of short Yagi aerials," *Journal of the Institution of Electrical Engineers — Part IIIA: Radiolocation*, Vol. 93, No. 3, 598–614, 1946.

[19] Brown, G. H., "Directional antennas," *Proceedings of the Institute of Radio Engineers*, Vol. 25, No. 1, 78–145, 1937.

[20] Viezbicke, P. P., *Yagi Antenna Design*, US Government Printing Office, 1976.

[21] Mailloux, R., "Antenna and wave theories of infinite Yagi-Uda arrays," *IEEE Transactions on Antennas and Propagation*, Vol. 13, No. 4, 499–506, 1965.

[22] Reid, D. G., "The gain of an idealized Yagi array," *Journal of the Institution of Electrical Engineers — Part IIIA: Radiolocation*, Vol. 93, No. 3, 564–566, 1946.

[23] Neff, H. P. and J. D. Tillman, "An omnidirectional circular antenna array excited parasitically by a central driven element," *Transactions of the American Institute of Electrical Engineers, Part I: Communication and Electronics*, Vol. 79, No. 2, 190–192, 1960.

[24] Schlub, R., J. Lu, and T. Ohira, "Seven-element ground skirt monopole ESPAR antenna design from a genetic algorithm and the finite element method," *IEEE Transactions on Antennas and Propagation*, Vol. 51, No. 11, 3033–3039, 2003.

[25] Schlub, R. and D. V. Thiel, "Switched parasitic antenna on a finite ground plane with conductive sleeve," *IEEE Transactions on Antennas and Propagation*, Vol. 52, No. 5, 1343–1347, 2004.

[26] Kawakami, H. and T. Ohira, "Electrically steerable passive array radiator (ESPAR) antennas," *IEEE Antennas and Propagation Magazine*, Vol. 47, No. 2, 43–50, 2005.

[27] Cai, Y., Z. Zhang, Y.-X. Sun, and D. Wu, "An ESPAR antenna with omnidirectional and steerable patterns for V2XApplications," in *2023 International Conference on Microwave and Millimeter Wave Technology (ICMMT)*, 1–3, Qingdao, China, May 2023.

[28] Ohira, T. and K. Gyoda, "Electronically steerable passive array radiator antennas for low-cost analog adaptive beamforming," in *Proceedings 2000 IEEE International Conference on Phased Array Systems and Technology (Cat. No.00TH8510)*, 101–104, Dana Point, CA, USA, May 2000.

[29] Rzymowski, M. and L. Kulas, "Two-row ESPAR antenna with simple elevation and azimuth beam switching," *IEEE Antennas*

*and Wireless Propagation Letters*, Vol. 20, No. 9, 1745–1749, 2021.

[30] Tillman, J. D., W. T. Patton, C. E. Blakely, and F. V. Schultz, "The use of a ring array as a skip range antenna," *Proceedings of the IRE*, Vol. 43, No. 11, 1655–1660, 1955.

[31] Kraus, J. D. and R. J. Marhefka, *Antennas For All Applications*, 1655–1660, McGraw-Hill, 2002.